# Accepted Manuscript


MESIA: Magnetic force-assisted electrochemical sandwich immunoassays for quantification of prostate-specific antigen in human serum

Hyundoo Hwang, Eunjong Choi, Seungmok Han, Yunsung Lee, Taehwa Choi, Mikyoung Kim, Haegong Shin, Jaesik Kim, Jaekyu Choi

PII: S0003-2670(19)30192-8

DOI: https://doi.org/10.1016/j.aca.2019.02.018

Reference: ACA 236582

To appear in: *Analytica Chimica Acta*

Received Date: 7 January 2019

Revised Date: 3 February 2019

Accepted Date: 9 February 2019

Please cite this article as: H. Hwang, E. Choi, S. Han, Y. Lee, T. Choi, M. Kim, H. Shin, J. Kim, J. Choi, MESIA: Magnetic force-assisted electrochemical sandwich immunoassays for quantification of prostate-specific antigen in human serum, *Analytica Chimica Acta*, https://doi.org/10.1016/j.aca.2019.02.018.

## Graphical abstract

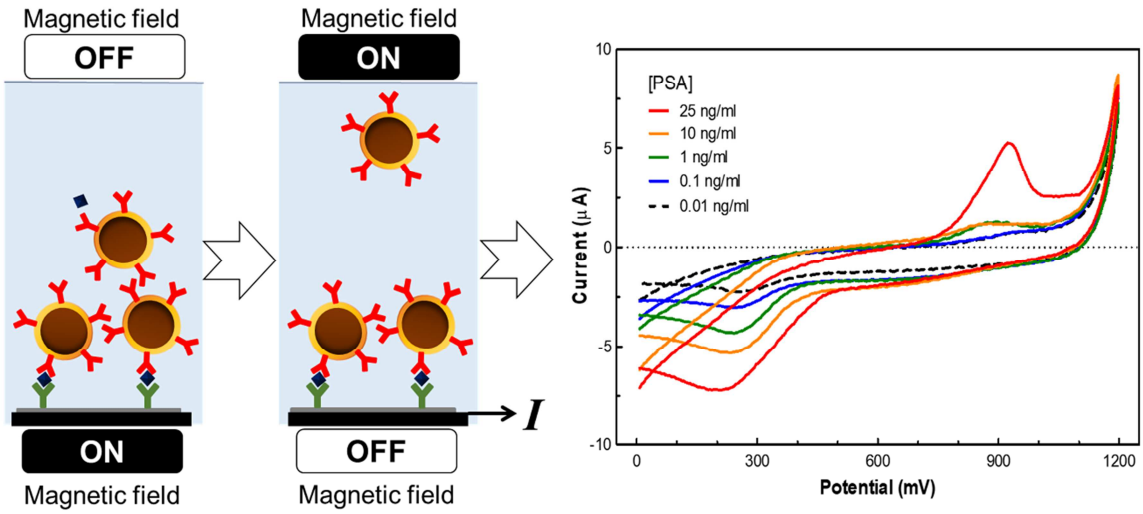

Revised Manuscript (Highlighted)

# MESIA: Magnetic force-assisted electrochemical sandwich immunoassays for quantification of prostate-specific antigen in human serum

Hyundoo Hwang*, Eunjong Choi, Seungmok Han, Yunsung Lee, Taehwa Choi, Mikyoung Kim, Haegong Shin, Jaesik Kim, Jaekyu Choi

*BBB Inc., 26 Samseong-ro 85-gil, Gangnam-gu, Seoul 06194, Republic of Korea*

***To whom correspondence should be addressed**: Hyundoo Hwang

Email: doo@bbbtech.com

**Abstract**

We propose a new immunoassay technique, called magnetic-force assisted electrochemical sandwich immunoassay (MESIA), where serum biomarkers can be determined by magnetic actuation and electrochemical detection of gold-coated iron oxide nanoparticles as probes for immunocomplex formation. In MESIA, neither washing buffer nor fluidic parts are necessary, because the formation of immunocomplexes and the removal of unbound probes are controlled by magnetic forces. Electrochemical pretreatment and measurement of the gold-coated magnetic probes allows highly sensitive, precise, and robust system for quantification of target analytes. Using MESIA, the concentration of prostate-specific antigen (PSA) in 10 μl of human serum is determined within 5 min. The limit of detection is 0.085 ng/mL, and the average coefficient of variance is 8.85% for five different PSA concentrations ranging from 0 to 25 ng/mL. This method shows good precision and reproducibility (<10%) and high correlation with cobas e 801 ($r$ = 0.997). We believe this technique to be useful in the development of a point-of-care testing platform for diagnosis and prognosis of various diseases, such as cancer, based on quantification of biomarkers in a drop of blood.

**Keyword**: prostate-specific antigen; electrochemistry; sandwich immunoassay; magnetic force; gold-coated magnetic nanoparticles

## 1. Introduction

Prostate cancer is currently the most prevalent form of cancer among men which prompts an immediate demand for early diagnosis. It has been shown that the presence or change in the level of specific biomarkers directly correlate with cancer development [1]. However, due to technical difficulties, a simple portable device to accurately measure these biomarkers has yet to be implemented. One possible approach to this conundrum could be the analysis of body fluids, such as blood or urine, specifically designed to detect prostate cancer biomarkers. Currently, serum prostate-specific antigen (PSA), a serine protease secreted exclusively by prostatic epithelial cells, is the most promising target for monitoring the progression of prostate cancer [2,3]. Various immunoassays which utilize electrochemistry [4], fluorescence spectroscopy [5,6], and chemiluminescence [7] have demonstrated the possibility of means to quantitatively measure PSA concentrations from blood samples. While these methods offer accurate results, they suffer from low throughput and high cost which restrain them for wider applications such as point-of-care testing (POCT).

For the last decade, the advancement of microfluidics has laid the groundwork for portable and automated POCT devices [8,9]. In the seminal work by Fan et al. an integrated blood barcode chip that not only is able to separate plasma from a few microliters of whole blood but also detects multiple protein markers by incorporating a fluorescence sandwich immunoassay has been demonstrated [10]. Moreover, the integrated blood barcode chip has been further improved to detect pM concentrations of more than 10 proteins from pinpricks of whole blood [11]. While the aforementioned microfluidic platforms provide highly sensitive measurements, they are not quite applicable for portable use due to the requirement of pre-stored buffers, reagents and their respective pumping devices.

To deal with this limitation, attempts have been made to eliminate mixing and buffer exchange steps. One such approach utilizes optically-induced electrokinetics to control the movement of fluids and probes using electric field distribution with pre-programmed image patterns. By controlling mixing and buffer exchange steps in the absence of any pumping devices, a rapid and automated sandwich immunoassays without any moving parts and human intervention was implemented [12]. Alternatively, Bruls and coworkers proposed an optomagnetic system which utilizes superparamagnetic nanoparticles such that the mixing and washing steps are be performed with a magnetic field within a stationary sample fluid [13]. However, both methods require optical components for detection. While these approaches successfully sidestepped the necessity for fluidic manipulation components, the optical components limit the implementation of POCT devices in practice, since they are relatively expensive and intolerant to environmental factors such as vibration and dust.

Our group has demonstrated the potential feasibility of the electrochemical approach by demonstrating protein biomarker detection via sandwich assays [14]. Compared to optical detection schemes, electrochemical approach may better suit the requirements for POCT devices due to its fast response time, low cost and simple instrumentation [15]. However, layers of molecules on the electrochemical sensor surface often interferes with efficient electron transfer from labels, resulting in low detection sensitivity. Recently, it has been shown that the sensitivity of the electrochemical immunoassay can be enhanced to the pM range by incorporating gold nanoparticle labeling along with a preoxidation step [16]. The preoxidation step utilizes the high solubility of gold nanoparticles under overpotential applications in chloride-rich conditions [17-20]. This works to an advantage because a

subsequent reduction step allows gold deposition to form on the electrode resulting in signal amplification.

In this paper, we introduce a new technique, called magnetic force-assisted electrochemical sandwich immunoassay (MESIA). In MESIA, all processes commonly required in conventional immunoassays, such as reaction and washing steps, are automatically controlled by magnetic force and the quantification of target analytes is performed by measuring the electrochemical signal. We incorporate gold-coated magnetic nanoparticles (AuMNPs) with anti-PSA antibodies such that the amount of gold present directly correlates to the amount of PSA in the electrochemical setup. We show that the electrical preoxidation of gold plays a key role in the sensitivity of the immunosensor. We believe that MESIA is able to meet the urgent demands of the POCT market, which has sought for a method enabling a simple handheld device that can offer automated, rapid, and accurate detection of disease markers from a drop of biological fluids. The application of MESIA is not only confined to PSA detection but would be scalable for any other protein biomarkers.

## 2. Experimental

### 2.1 Materials

Gold(III) chloride trihydrate ($HAuCl_4 \cdot 3H_2O$), Tween-20, human sera, and all buffer solutions were purchased from Sigma Aldrich (St. Louis, USA). Carboxymethyl dextran (CMD) was purchased from TdB Consultancy (Uppsala, Sweden). 1-ethyl-3-(3-dimethylaminopropyl)-carbodiimide (EDC), N-hydroxysulfosuccinimide (sulfo-NHS), and MES buffer were purchased from Thermo Fisher Scientific (Walthan, USA). Bovine serum albumin (BSA) was purchased from Bovogen Biologicals (Melbourne, Australia). The protein thiolation kit was purchased from Novus biologicals (Littleton, USA). Antibodies and magnetic nanoparticles (MNPs) were purchased from Hytest (Turku, Finland) and Micromod (Rostock, Germany), respectively. All the aqueous solutions were prepared in deionized (DI) water (18.2 MΩ·cm), which was obtained from a Milli-Q water-purification system. Patient samples were collected from patients treated at Seoul National University Bundang Hospital with appropriate Institutional Review Board (IRB) approval.

### 2.2 Instruments

Cyclic voltammetry (CV) and electrochemical impedance spectroscopy (EIS) were conducted using a Parstat MC potentiostat (AMETEK Inc., Berwyn, PA). The proper synthesis of antibody-immobilized AuMNPs was validated by scanning electron microscopy (SEM) (Carl Zeiss, Oberkochen, Germany) and UV-Vis spectrometer (Molecular Devices, San Jose, CA). The magnetic actuation of the antibody-immobilized AuMNPs was performed

using a custom-built magnet control system, in which the movement of two permanent magnets was precisely controlled by step motors.

### 2.3 Preparation of electrochemical sensors

Screen-printed carbon electrodes (SPCEs) were prepared by printing carbon as the working and counter electrodes and Ag/AgCl as the reference electrode. In order to immobilize the anti-PSA antibodies onto the working electrode, first of all, 4 µl of 0.1 mg/ml CMD solution prepared in DI water was loaded on the working electrode and incubated overnight at the room temperature in a humid chamber. After washing of any residual CMD solution, 4 µl of 0.1 M EDC and 0.1 M sulfo-NHS prepared in 0.1M MES buffer (pH 4.7) was loaded on the working electrode and incubated at the room temperature for 1 h to activate the carboxyl group of CMD. The working electrode was washed and immediately treated with 0.05 mg/ml monoclonal anti-PSA antibody solution prepared in 10 mM PBS buffer for 2 h. The antibody-immobilized SPCEs were then sequentially dipped and agitated in 1% BSA solution for 1 h. Finally, the electrodes were washed with DI water and stored at 4°C until needed.

### 2.4 Preparation of gold-coated magnetic nanoparticles

0.5 mg of MNP (250 nm dia.) from the stock solution was suspended in 10 mL of 10 mM phosphate buffer (PB). The solution was sonicated for 10 min and stirred in a dark room. We gently added 1 ml of 1% sodium citrate prepared in 10 mM PB and increased the temperature to 100°C. Once the solution reached 100°C, we added 0.2 ml of 10 mM

$HAuCl_4 \cdot 3H_2O$ to seed gold nanoparticles on the surface of MNPs. The solution left on the stirrer for an additional 10 min. The AuMNPs were washed 2 times with 10 mM PB and finally resuspended with 0.5 ml of 10 mM PB.

### 2.5 Immobilization of antibodies on AuMNPs

To effectively immobilize monoclonal anti-PSA antibodies onto the AuMNPs, we introduced a free thiol group to the antibodies by using a protein thiolation kit. We then mixed 10 μg of thiolated antibodies with 0.5 ml of AuMNP solution and rotated at 25°C for 1 h. The antibody-immobilized AuMNP probes were gathered at the bottom of the vial, using a magnet, after which the supernatant was replaced with 1% BSA solution. The solution is further mixed on a rotator for 1 h, then the antibody-immobilized AuMNP probes were washed with 10 mM PB three times. Finally, 1 mg/ml AuMNPs was stored at 4°C until further use.

### 2.6 Electrochemical measurements

Prior to the quantitative measurements, a pretreatment step in PBS was conducted by applying 1.5 V for 10 s and scanning potential from 1.5 to 0 V at 0.1 V/s scan for electrochemical preoxidation and reduction of the gold nanoparticles on MNPs, respectively. Subsequently, a CV measurement was conducted by potential cycling from 0.0 to 1.2 V at 0.1 V/s to obtain CV curves for quantification of bound AuMNPs. The cathodic and anodic peaks in CV were analyzed using a custom software written in JAVA.

### 2.7 Quantification of prostate-specific antigen in human serum

In order to perform all-in-one immunoassays to detect PSA in human serum with MESIA, human blood sera with 0.5 M NaCl at desired PSA concentrations were prepared. 5 × $10^7$ AuMNP probes were added to 10 μl of PSA-spiked serum sample, followed by loading the mixture on the SPCE sensor. During the reaction process, the AuMNP probes were repeatedly pulled toward and away from the working electrode by continuously moving permanent magnets above and under the SPCEs device, respectively. The AuMNP probes were contacted to the antibody-immobilized working electrode for 2 s with the interval of 2 s during the process to induce the formation of immunocomplexes. After 3 min of reaction, unbound AuMNP probes were removed by putting a permanent magnet at the top for 25 s. The immunocomplexes formed on the electrode were quantified via CV scan after the pretreatment step. The magnetic reaction and washing processes were automatically performed using a custom electromechanical system.

### 2.8 Clinical sample analyses

All patient serum samples were collected following approval by the Seoul National University Bundang Hospital Institutional Review Board (IRB). For comparison of the methods, PSA concentration of the patient samples were analyzed using cobas e 801 (Roche Diagnostics, Risch-Rotkreuz, Switzerland) and the proposed method at the same time. Passing-Bablock regression analysis was conducted to define the Pearson correlation coefficient.

## 3. Results and Discussion

A schematic diagram of MESIA, which is a sandwich immunoassay platform utilizing magnetic fields and electrochemistry for quantification quantitatively measure analyte concentrations in the absence of fluidic manipulation components and pre-stored washing buffers, is shown in Figure 1a. The magnetic probes used in this platform are designed such that detection antibodies, which capture analytes, are conjugated to gold-coated iron oxide nanoparticles. The AuMNPs are highly maneuverable via magnetic fields and the gold nanoparticles coated on the MNPs elicit strong electrochemical signals. The AuMNP probes can form sandwich immunocomplexes on the antibody-immobilized electrode surface via analytes. The antibody-antigen reactions for the formation of immunocomplexes and the removal of unbound probes are controlled and accelerated by external magnetic fields. Finally, the amount of analytes is quantified by measuring the electrochemical signals from the AuMNPs bound onto the sensor surface. Here we applied this platform for the quantification of PSA in human serum. First of all, the sample is mixed with AuMNP probes (Figure 1b). Then magnetic fields are applied such that magnetic probes are interacted with the target analytes and form immunocomplexes on the surface of the working electrode (Figure 1c). After sufficient reaction, the unbound magnetic probes are cleared off of the working electrode by applying a magnetic field (Figure 1d). We then apply high electrical potential to induce electrochemical oxidation of gold on the bound probes (Figure 1e), followed by CV scan for the quantitative measurement (Figure 1f).

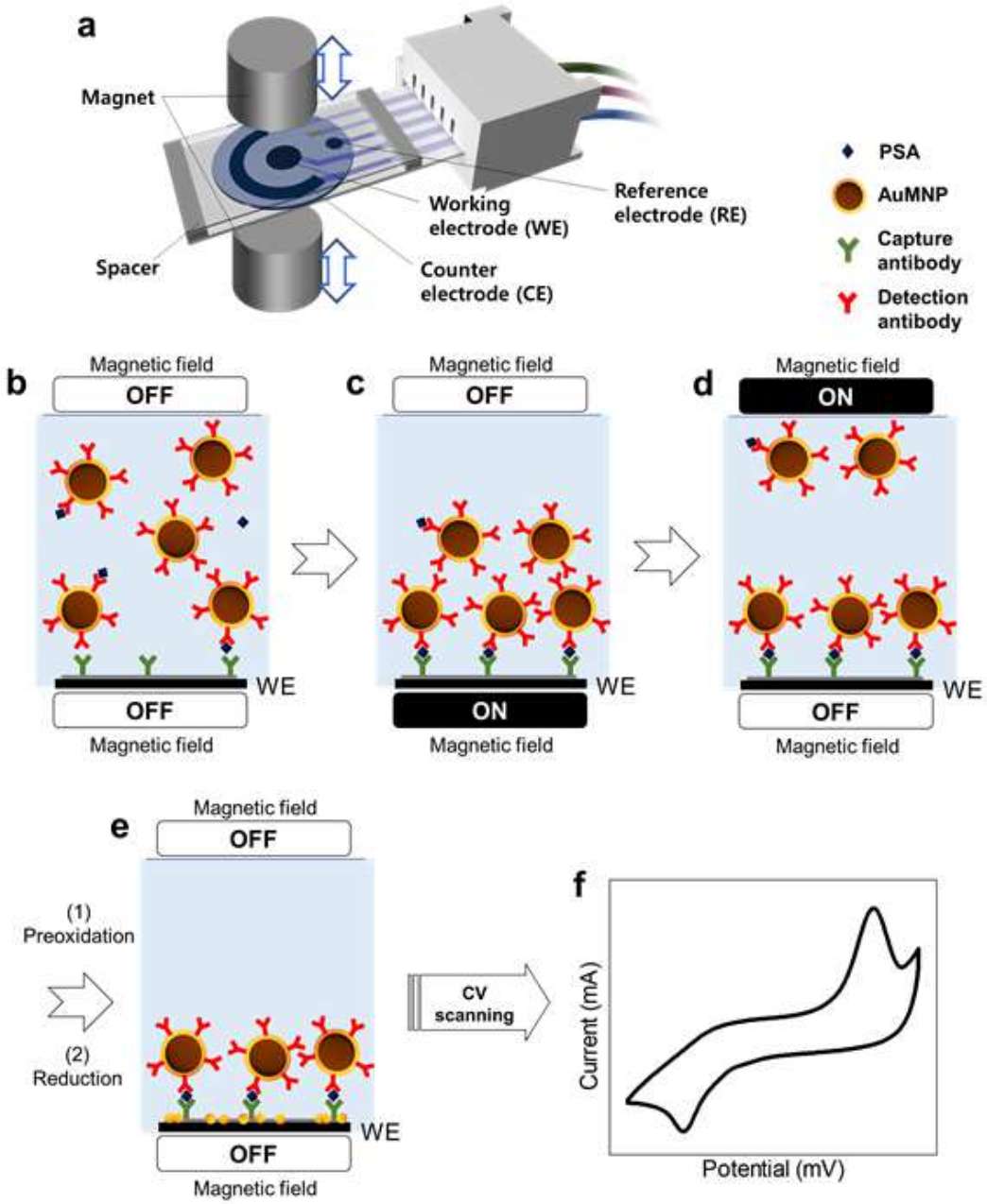


**Figure 1.** Schematic diagram of magnetic force-assisted electrochemical sandwich immunoassay. **(a)** Magnetic actuation and electrochemical detection of nanoprobes forming sandwich immunocomplexes allow fast, highly sensitive, robust, and low-cost immunoassays of serum biomarkers in a stationary fluid. In detail, **(b)** gold-coated magnetic nanoparticles (AuMNPs) conjugated with detection antibodies interact with the target analytes in a drop of

human serum. **(c)** The AuMNPs are controlled by a magnetic force to form immunocomplexes on the working electrode of electrochemical sensor. **(d)** After the reaction step, unbound probes are removed by a magnetic force. **(e)** For highly sensitive detection of the AuMNPs forming immunocomplexes, which correlates with the concentration of target analytes, electrochemical pretreatment is conducted. **(f)** Finally, the amount of target analytes is quantitatively measured by electrochemical methods such as cyclic voltammetry.

### 3.1 Characterization of gold-coated magnetic nanoparticle (AuMNP) probes

The electrochemically-labelled magnetic nanoprobes used in MESIA were prepared by coating gold nanoparticles and anti-PSA antibodies onto iron oxide nanoparticles, as electrochemical redox labels and the analyte-capturing molecules, respectively. Because the strength and reproducibility of redox signals from CV scan directly correlates with the detection performances, our system relies greatly upon the amount of gold present on the MNP.

Comparison between back-scattered electron SEM images of bare MNPs and AuMNPs clearly depict gold nanoparticles, of which size ranges from ~50 to ~80 nm, present on the MNP surface (Figures 2a and 2b). Furthermore, the UV-Vis spectra of the AuMNPs present a definitive peak at ~550 nm, representing gold seeds (~50 to ~100 nm) [21], compared to the monotonically decreasing spectrum of bare MNPs (Figure 2c).

Since MESIA utilizes the electrochemical redox properties of gold, it is crucial to confirm the redox peaks of the AuMNPs prior to any further experiments. Therefore, we

prepared a PBS solution containing AuMNP probes and magnetically gathered them onto the working electrode and ran a CV scan from 0.0 to 1.2 V at 0.1 V/s. However, the redox curve of AuMNPs did not exhibit any appreciable redox peak (Figure 2d). It is possible that the lack of signal is due to the lack of accessibility of the gold nanoparticles, residing on the MNPs, and the carbon electrode caused by the thickness of molecular layer on the electrode and the size of MNPs (Figure 1b).

To deal with this problem, we applied a pretreatment step for the electrochemical preoxidation and reduction of gold prior to the quantitative measurement by CV. The pretreatment step consists of an application of high voltage which strips the gold nanoparticles followed by an immediate lower voltage which reduces the oxidized gold ions onto the working electrode. Previous studies have reported successful oxidization of gold nanoparticles labeled on the antibodies and subsequent reduction onto the working electrode in the presence of chloride ion-providing reagents [18-20].

Here we applied 1.5 V for 10 s for the electrical oxidation of gold, followed by a potential scan from 1.5 to 0.0 V at 0.1 V/s for reduction. After this pretreatment step, a CV scan from 0.0 to 1.2 V at 0.1 V/s was conducted to confirm the oxidation and reduction signals of gold. Consequently, we could obtain redox peaks strong enough to be utilized for the assays at around 0.25 and 1.0 V, as shown in Figure 2d. We could not find any distinguishable peaks from bare MNPs and PBS despite the same pretreatment step (Figure 2e), thus we can deduce that the peaks are from the oxidation and reduction of gold. These results collectively support the usefulness of AuMNPs that we synthesized as the magnetic probes for MESIA.

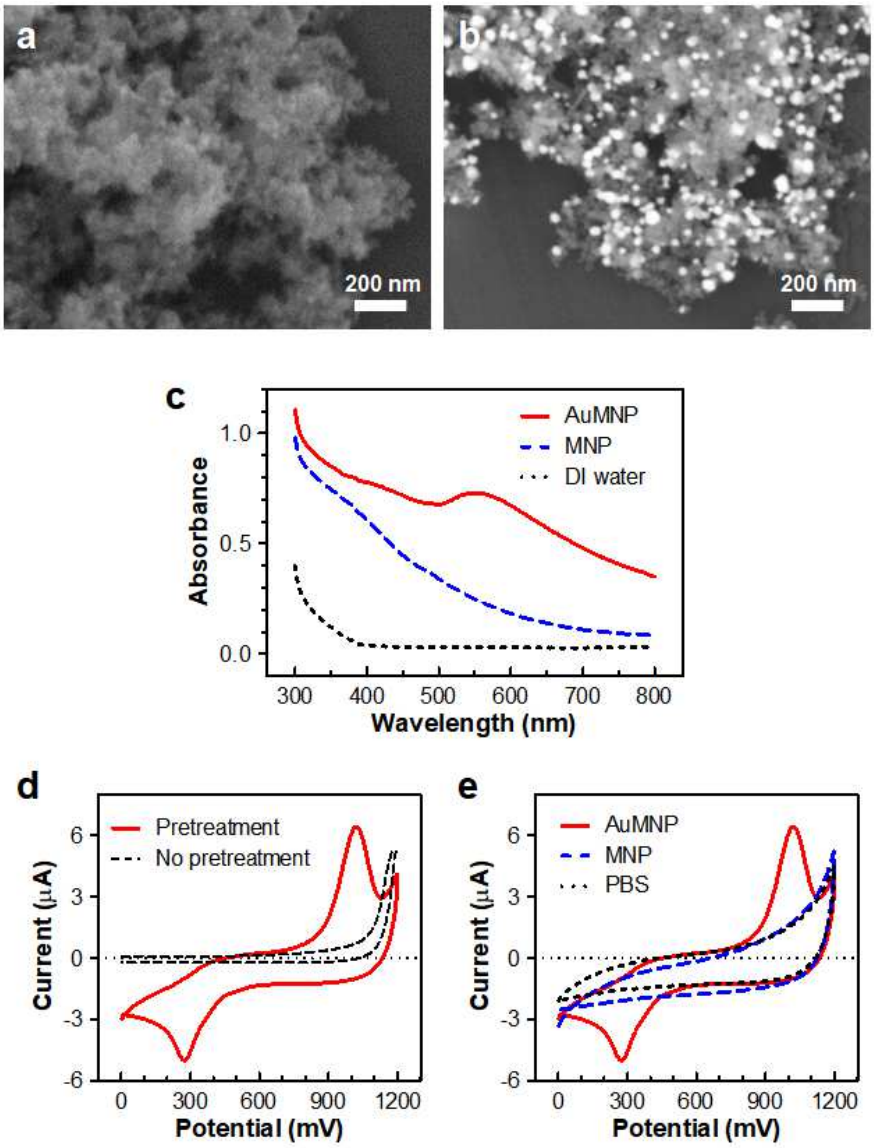


**Figure 2.** Characterization of gold-coated magnetic nanoparticles (AuMNPs). Scanning electron microscopic images of **(a)** bare magnetic nanoparticles (MNPs) and **(b)** AuMNPs. **(c)** UV-Vis spectra of bare MNPs, AuMNPs, and DI water. **(d)** Cyclic voltammograms of AuMNPs before and after the electrochemical pretreatment step. **(e)** Cyclic voltammograms of AuMNPs, MNPs, and PBS solution, measured after the pretreatment step.

### 3.2 Characterization of sandwich complex formation

Each process for the fabrication of anti-PSA antibody-based electrochemical sensors and the sandwich assays was verified by EIS. The sensing electrodes were prepared by treating the working electrode surface with CMD, followed by immobilization of anti-PSA capture antibodies via sulfo-NHS cross-linker. During the assay, PSA molecules are recognized by the antibodies on the electrode and the AuMNP probes, respectively, resulting in the formation of sandwich complexes on the working electrode. To confirm whether the antibodies and PSA bind together and form the sandwich complexes, the EIS measurements were performed for each binding process (Figure 3a). The charge transfer resistance, $R_{ct}$, was measured at each step in the presence of 3 mM $[Fe(CN)_6]^{3-}$ in $KNO_3$ as shown in Figure 3b. The $R_{ct}$ gradually increased from 8.82 kΩ to 36.8 kΩ, 53.3 kΩ, and 72.4 kΩ after the antibody immobilization, the recognition of PSA, and the binding of AuMNP probes, respectively. The increase in $R_{ct}$ after each step implies that molecular layers have been stacked on the working electrode, which interfere with the charge transfer and hinder the access of redox agent to the electrode surface.

To validate the feasibility of this assay, we conducted CV measurements in the presence and absence of PSA. We first incubated the antibody-immobilized electrodes with 0 and 10 ng/mL PSA for 1 h at room temperature, and washed out unbound PSA molecules using a PBS solution. The magnetic probes were then loaded and performed the magnetic reaction process for 3 min. Thereafter, the unbound AuMNP probes were removed using a magnet or a PBS washing buffer. After the pretreatment step, CVs were measured as shown in Figures 4a and 4b. The results clearly showed that while no appreciable redox peak was observed after washing in the absence of PSA (Figure 4a), a distinct peak is shown in the

presence of 10 ng/mL PSA (Figure 4b), regardless of the washing method – a magnet or a washing buffer. These results indicate that the immobilization of capture antibodies and the binding processes of the sandwich immunoassays are properly functioning, and the redox peaks from gold on the MNP probes can be directly measured in our electrochemical sandwich immunoassay system. These results also suggest not only is it possible to form the sandwich immunocomplexes on the working electrode, but also that the magnetic washing is as effective as conventional flow washing

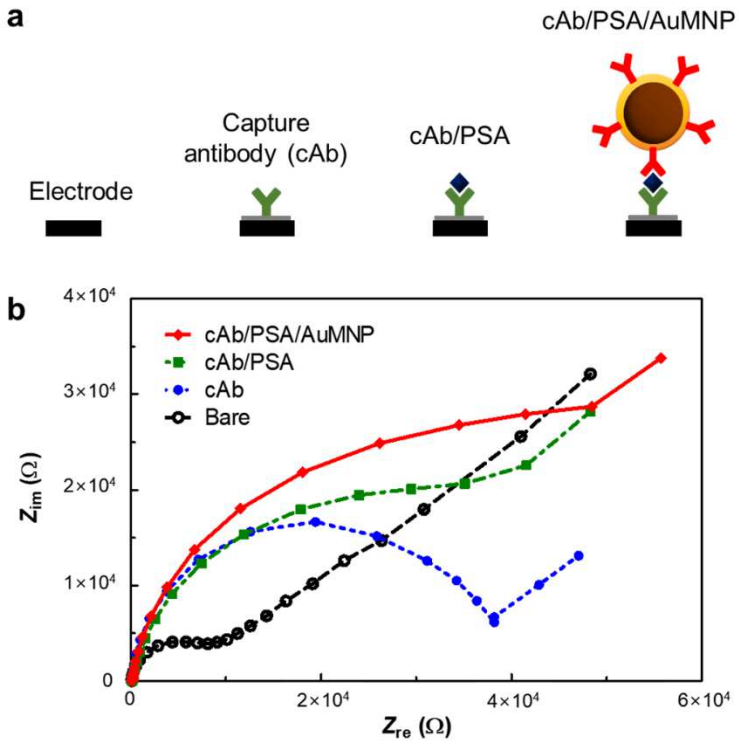


**Figure 3.** Electrochemical impedance spectroscopy (EIS) analysis of the formation of immunocomplexes. **(a)** Processes of forming immunocomplexes on the working electrode surface for the EIS analysis. **(b)** EIS spectra of carbon electrode before and after capture antibody (cAb) immobilization, prostate-specific antigen (PSA) binding, and immunocomplex formation with gold-coated magnetic nanoparticle (AuMNP).

### 3.3 Optimization of reaction and washing times

We conducted all-in-one assay by adding AuMNP probes to PSA sample solution. After loading the mixture into a SPCE sensor, the MESIA processes, which include the magnetic control of immunocomplex formation, and the electrochemical analysis for quantification, were automatically performed.

In order to obtain the optimal reaction and washing conditions, we further varied the duration of each step, and measured the cathodic peak current. The time for magnetic washing of unbound AuMNP probes was examined from 0 to 30 s. The response current was decreased as the washing time increases, and it reached steady state at 25 s (Figure 4c). Thus, the washing time was chosen to be 25 s. The reaction time of AuMNPs to the antibodies on the working electrode also varied from 0 to 5 min as shown in Figure 4d. The response was increased gradually and reached steady state at 3 min. Thus, the optimal reaction time was chosen to be 3 min.

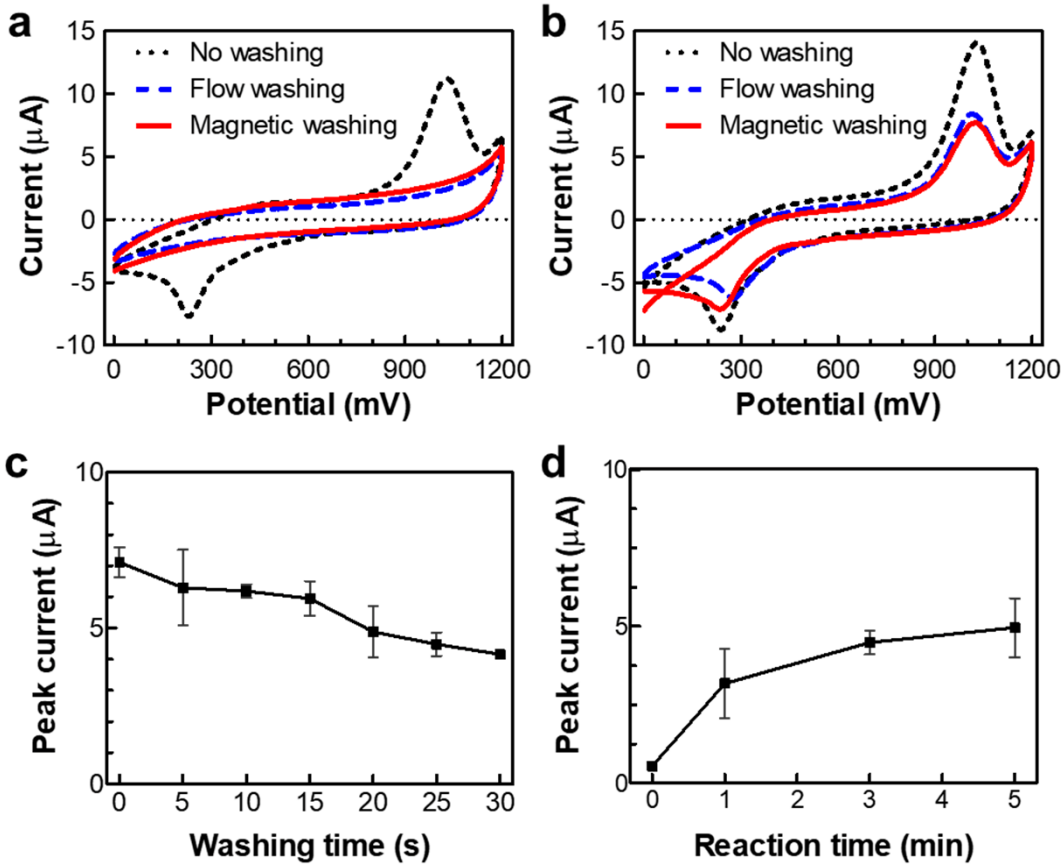


**Figure 4.** Validation and optimization of magnetic control of immunoreactions and washing processes. Cyclic voltammograms measured after magnetic removal of nanoprobes in the **(a)** absence and **(b)** presence of 10 ng/mL PSA, which are consistent with those after conventional flow washing. Intensities of cathodic peak currents of CV from the assays of PSA according to the magnetic **(c)** washing and **(d)** reaction times.

To validate the system, we conducted the experiments with various PSA concentrations from 0 to 25 ng/mL and obtained CV curves (Figure 5a). The results show a clear increase in peak currents in accordance with the PSA concentrations. In particular, the cathodic peak current was significantly correlated with the PSA concentration as shown in Figure 5b ($R^2$ = 0.96). These results suggest that the MESIA system can be utilized for quantification of PSA.

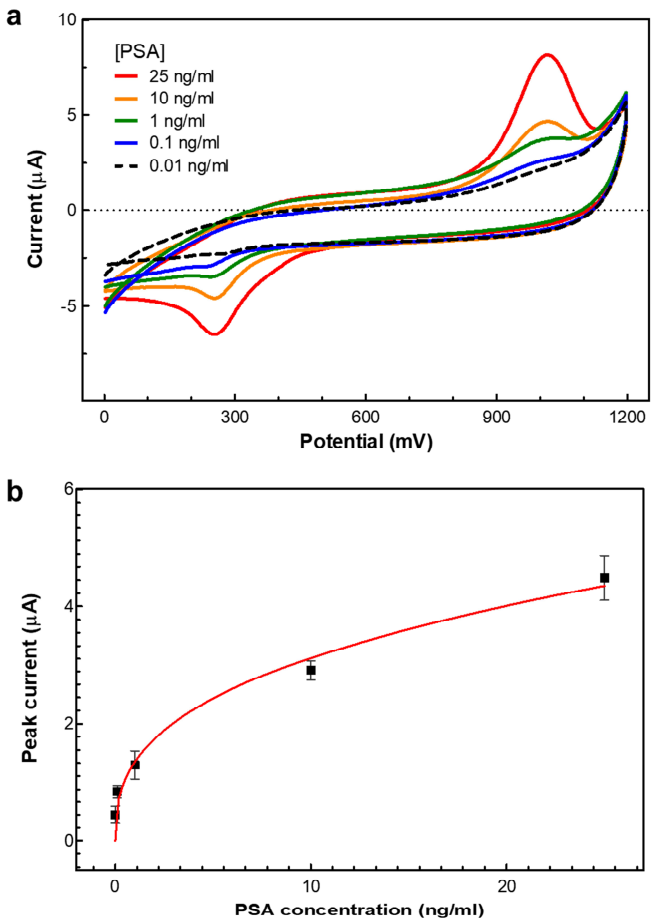


**Figure 5.** Determination of PSA in PBS solution using magnetic force-assisted electrochemical sandwich immunoassays. (a) Cyclic voltammograms for various concentrations of PSA from 0 to 25 ng/mL. (b) Cathodic peak currents vs. PSA concentration. Mean ± standard deviation ($n \geq 3$). The fitting curve is also plotted ($R^2$ = 0.96).

### 3.4 Analysis of human serum

We applied the MESIA for the determination of PSA in human serum. To confirm whether the change in solution affects the electrochemical responses of AuMNPs, CV curves from assays of 10 ng/mL PSA in PBS solution and human serum were compared to each other (Figure 6). To our surprise, although the pretreatment step was conducted for both cases, it was not possible to find any appreciable redox peaks in the assays with human serum, while we could observe clear redox peaks in the assays with PBS solution. When we performed the assays with PBS solution with serum proteins including albumin, we could obtain the same voltammogram with that of serum, which has no appreciable redox peaks (data not shown). This implies that electroactive serum proteins might interfere with efficient oxidation and reduction of gold in serum during the pretreatment step.

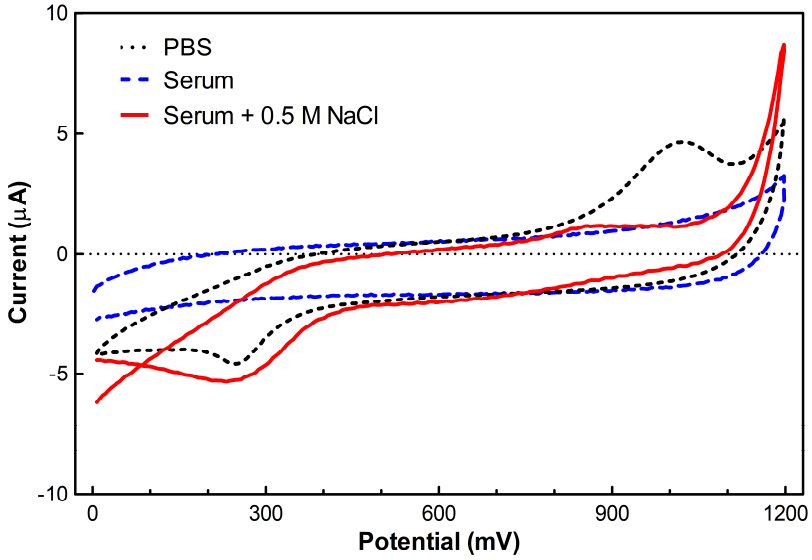


**Figure 6.** Cyclic voltammograms in the assays of 10 ng/mL PSA in PBS solution, human sera. Anodic and cathodic peaks of gold were observable when NaCl was added to human serum.

To deal with this issue, 0.5 M NaCl was added to human serum, as it has been known that chloride-rich conditions induce high solubility of gold nanoparticles under overpotential applications [17-20]. As we expected, clear redox peaks were observable in CV from the assays of PSA in serum with 0.5 M NaCl, as shown in Figure 6. We were convinced that the peaks are due to the electrochemical oxidation and reduction of AuMNP probes, not NaCl or others, because the peak currents increased as the PSA concentration in serum increased (Figure 7a).

In the assays with human sera of various PSA concentrations from 0 to 25 ng/mL, the strength of cathodic peak at around 0.25 V increased as the concentration of PSA increased (Figure 7a). The measured values of cathodic peak currents highly correlated with the PSA concentration as shown in Figure 7b ($R^2$ = 0.97). The limit of detection for PSA was 0.085 ng/mL and the average coefficient of variance was 8.85%. There was no high dose hook effect and the coefficient of variance were still less than 10% up to 1,000 ng/mL of PSA, but the cathodic peak current gradually decreased when the PSA concentration increased to 20,000 ng/mL. However, the signal intensity at 20,000 ng/mL PSA was still higher than that at 30 ng/mL, which is the upper limit of measuring range that we claim in this study. When we tested the sensors after storing them under controlled humidity (~20% RH) and temperature (~4℃) conditions for more than 3 months, they showed consistent performances. Considering the fact that clinical cut-off value of PSA ranges from 2.5 to 4.0 ng/mL, our results suggest that the MESIA would be potentially be applicable for future prostate cancer diagnosis and prognosis based on blood tests.

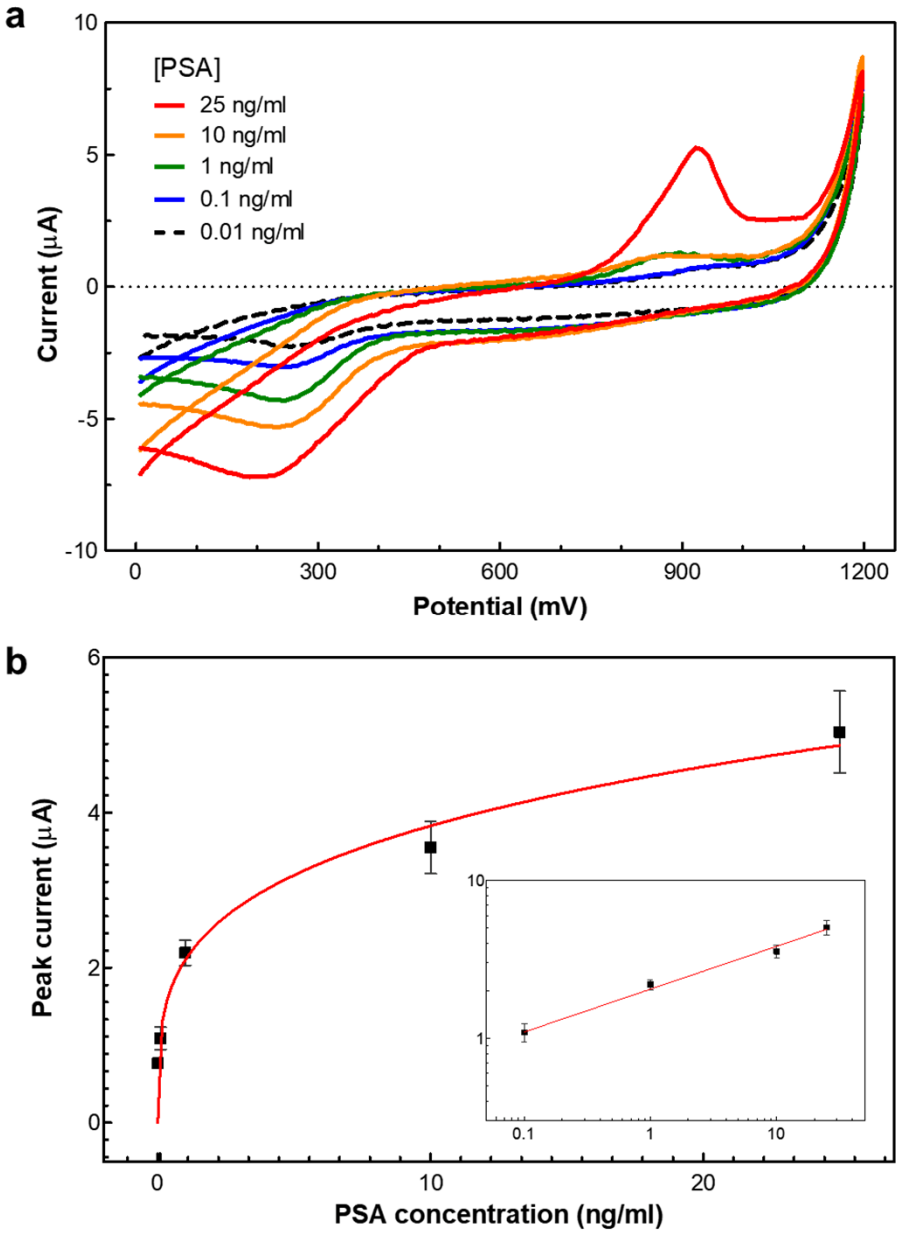


**Figure 7.** Determination of PSA in human serum using magnetic force-assisted electrochemical sandwich immunoassays. **(a)** Cyclic voltammograms for various concentrations of PSA from 0 to 25 ng/mL. **(b)** Cathodic peak currents vs. PSA concentration. Mean ± standard deviation ($n \geq 3$). The inset shows a log plot of the data. The fitting curve is also plotted ($R^2 = 0.97$). The limit of detection was calculated to be 0.085 ng/mL.

### 3.5 Clinical sample analyses

We confirmed recovery, precision and reproducibility of the MESIA-based quantitative PSA detection method using clinical sera. PSA at a known concentration was spiked into female serum mixed with 0.5 M NaCl, and the electrochemical signal was measured with MESIA to compare the recovery rate between the values. Four concentrations were selected to cover both normal and abnormal samples between 0 and 30 ng/mL of PSA. All values were included within the aimed recovery rate range (≥ 95%) (See Table 1). In addition, a precision test for serum PSA measurements was performed using four patient samples in different PSA range (0.1 to 1, 1 to 5, 5 to 10, and 10 to 30 ng/mL). 3 different lots of the MESIA devices were prepared and tested the 3 replicates during 2 runs each day for 5 days, and within-run, between-run, between-day, and between-lot precision data were investigated as summarized in Table 2. The MESIA-based PSA assays showed a precision performance of less than 10% CV except the within-run precision (13.5%) at the lowest concentration sample (See Table 2).

Table 1. Spiked PSA recovery data of the MESIA-based PSA assays

| Added PSA (ng/mL) | Observed PSA (ng/mL) | Recovery (%) |
|---|---|---|
| 1.03 | 1.02 | 99.03 |
| | 1.00 | 97.09 |
| | 1.01 | 98.06 |
| 5.60 | 5.60 | 99.82 |
| | 5.42 | 96.79 |
| | 5.55 | 99.11 |
| 13.24 | 12.98 | 98.04 |
| | 13.21 | 99.77 |
| | 13.32 | 100.6 |
| 24.92 | 24.89 | 99.98 |
| | 24.13 | 96.83 |
| | 25.11 | 100.8 |

Table 2. Precision data for the MESIA-based PSA assays

| Sample number | Mean PSA (ng/mL) | Coefficient of variation (%) | | | |
|---|---|---|---|---|---|
| | | Within-run | Between-run | Between-day | Between-lot |
| 1 | 0.264 | 13.5 | 7.5 | 5.1 | 6.5 |
| 2 | 1.02 | 8.6 | 1.6 | 1.6 | 5.8 |
| 3 | 5.56 | 5.4 | 6.8 | 6.8 | 7.1 |
| 4 | 29.1 | 6.1 | 7.6 | 5.5 | 3.0 |

The PSA concentrations in 16 patient serum samples measured by the MESIA were compared with those measured by cobas e 801, which is a reference device (See Figure 8). The linear regression analysis yielded a slope of 1.04 and y-intercept of -0.124 ng/mL ($r$ = 0.997) in the range from 0.103 to 29.1 ng/mL. These results imply that MESIA could be applied for qualitative analysis of PSA in human blood for diagnosis and management of prostate cancer in the clinical practices.

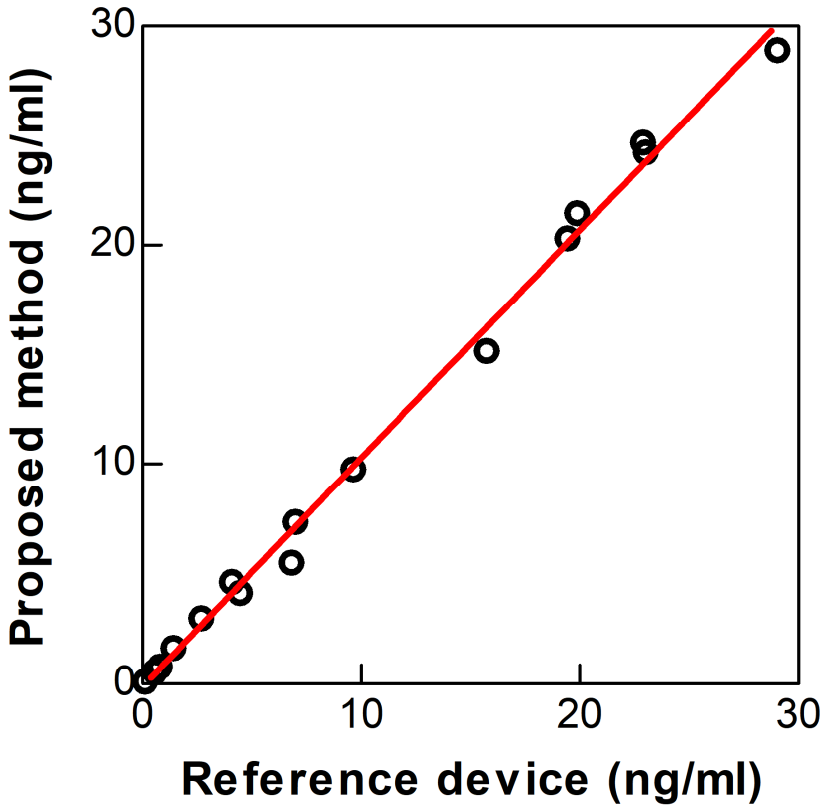


**Figure 8.** Comparison of the PSA values of 16 patient samples measured by the proposed method with those measured by a reference device, cobas e 801 ($r$ = 0.997, $y$ = 1.04$x$ - 0.124)

## 4. Conclusion

In this research, we present a new immunoassay technique, called MESIA, in which AuMNPs are utilized as probes for electrochemical sandwich immunoassays of PSA. In MESIA, magnetic control of the formation of immunocomplexes and removal of unbound probes enables rapid and efficient interactions among the antibodies and target analytes in a tiny volume of stationary fluid. In addition, electrochemical measurement rejects the intrinsic limitations of optical detection system, such as high cost, intolerance to vibration, and high sensitivity to ambient dust. Using the MESIA, we could quantitatively determine PSA in 10 μl of human serum with the limit of detection of 0.085 ng/mL within 5 min. The MESIA showed satisfactory precision and reproducibility, as well as high correlation with cobas e 801 within the measuring range (0.085 to 30 ng/mL). While the MESIA system was applied for determining PSA in this study, the MESIA would also be useful for quantification of various biomarkers in bodily fluid samples. Due to the advantages that the MESIA offers, we believe that practical implementation for real life usage as a handheld POCT device would be achievable in the near future.

## Acknowledgements

This work was supported by the Ministry of Trade, Industry and Energy, Republic of Korea (No. 10067197). This research was also supported by the National Research Foundation funded by the Korean government (NRF-2017M3A9E2062212).

## Conflict of interest

The authors declare that there are no conflicts of interest.

**References**

[1] Chatterjee, S.K., Zetter, B.R., 2018. Future Oncol. 1, 37-50.

[2] Stamey, T. A., Yang, N., Hay, A.R., McNeal, J.E., Freiha, F.S., Redwine, E., 1987. N. Engl. J. Med. 317, 909-916.

[3] Catalona, W.J., Smith, D.S., Ratliff, T.L., Dodds, K.M., Coplen, D.E., Yuan, J.J.J., Petros, J.A., Andriole, G.L., 1991. N. Engl. J. Med. 324, 1156-1161.

[4] Wang, H., Zhang, Y., Yu, H., Wu, D., Ma, H., Li, H., Du, B., Wei, Q., 2013. Anal. Biochem. 434, 123-127.

[5] Liu, D., Huang, X., Wang, Z., Jin, A., Sun, X., Zhu, L., Wang, F., Ma, Y., Niu, G., Hight Walker, A.R., Chen, X., 2013. ACS Nano 7, 5568-5576.

[6] Matsumoto, K., Konishi, N., Hiasa, Y., Kimura, E., Takahashi, Y., Shinohara, K., Samori, T., 1999. Clin. Chim. Acta 281, 57-69.

[7] Matsuya, T., Tashiro, S., Hoshino, N., Shibata, N., Nagasaki, Y., Kataoka, K., 2003. Anal. Chem. 75, 6124-6132.

[8] Yetisen, A.K., Akram, M.S., Lowe, C.R., 2013. Lab Chip 13, 2210-2251.

[9] Jung, W., Han, J., Choi, J.-W., Ahn, C.H., 2013. Microelectron. Eng. 132, 46-57.

[10] Fan, R., Vermesh, O., Srivastava, A., Yen, B.K.H., Qin, L., Ahmad, H., Kwong, G.A., Liu, C.-C., Gould, J., Hood, L., Heath, J.R., 2008. Nat. Biotechnol. 26, 1373-1378.

[11] Wang, J., Ahmad, H., Ma, C., Shi, Q., Vermesh, O., Vermesh, U., Heath, J., 2010. Lab Chip 10, 3157-3162.

[12] Hwang, H., Chon, H., Choo, J., Park, J.-K., 2010. Anal. Chem. 82, 7603-7610.

[13] Bruls, D.M., Evers, T.H., Kahlman, J.A., van Lankvelt, P.J., Ovsyanko, M., Pelssers, E.G., Schleipen, J.J., de Theije, F.K., Verschuren, C.A., van der Wijk, T., van Zon, J.B., Dittmer, W.U., Immink, A.H., Nieuwenhuis, J.H., Prins, M.W., 2009. Lab Chip 9, 3504-3510.

[14] Chung, S., Moon, J.-M., Choi, J., Hwang, H., Shim, Y.-B., 2018. Biosens. Bioelectron. 117, 480-486.

[15] Kokkinos, C., Economou, A., Prodromidis, M.I., 2016. Trends Anal. Chem. 79, 88-105.

[16] Kokkinos, C., Economou, A., 2017. Anal. Chim. Acta 961, 12-32.

[17] Lim, S.A., Yoshikawa, H., Tamiya, E., Yasin, H.M., Ahmed, M.U., 2014 RSC Advances 4, 58460-58466.

[18] Ding, L., Bond, A.M., Zhai, J., Zhang, J., 2013. Anal. Chim. Acta 797, 1-12.

[19] Koutarou, I., Miyuki, C., Kagan, K., Naoki, N., Teruko, Y., Tatsuro, E., Eiichi, T., 2008. Electroanal. 20, 14-21.

[20] Kim, M., Kim, J., 2014. Langmuir 30, 4844-4851.

[21] Haiss, W., Thanh, N.T.K., Aveyard, J., Fernig, D.G., 2007. Anal. Chem. 79, 4215-4221.

**FIGURE CAPTIONS:**

**Figure 1.** Schematic diagram of magnetic force-assisted electrochemical sandwich immunoassay. **(a)** Magnetic actuation and electrochemical detection of nanoprobes forming sandwich immunocomplexes allow fast, highly sensitive, robust, and low-cost immunoassays of serum biomarkers in a stationary fluid. In detail, **(b)** gold-coated magnetic nanoparticles (AuMNPs) conjugated with detection antibodies interact with the target analytes in a drop of human serum. **(c)** The AuMNPs are controlled by a magnetic force to form immunocomplexes on the working electrode of electrochemical sensor. **(d)** After the reaction step, unbound probes are removed by a magnetic force. **(e)** For highly sensitive detection of the AuMNPs forming immunocomplexes, which correlates with the concentration of target analytes, electrochemical pretreatment is conducted. **(f)** Finally, the amount of target analytes is quantitatively measured by electrochemical methods such as cyclic voltammetry.

**Figure 2.** Characterization of gold-coated magnetic nanoparticles (AuMNPs). Scanning electron microscopic images of **(a)** bare magnetic nanoparticles (MNPs) and **(b)** AuMNPs. **(c)** UV-Vis spectra of bare MNPs, AuMNPs, and DI water. **(d)** Cyclic voltammograms of AuMNPs before and after the electrochemical pretreatment step. **(e)** Cyclic voltammograms of AuMNPs, MNPs, and PBS solution, measured after the pretreatment step.

**Figure 3.** Electrochemical impedance spectroscopy (EIS) analysis of the formation of immunocomplexes. **(a)** Processes of forming immunocomplexes on the working electrode surface for the EIS analysis. **(b)** EIS spectra of carbon electrode before and after capture antibody (cAb) immobilization, prostate-specific antigen (PSA) binding, and immunocomplex formation with gold-coated magnetic nanoparticle (AuMNP).

**Figure 4.** Validation and optimization of magnetic control of immunoreactions and washing processes. Cyclic voltammograms measured after magnetic removal of nanoprobes in the **(a)** absence and **(b)** presence of 10 ng/mL PSA, which are consistent with those after conventional flow washing. Intensities of cathodic peak currents of CV from the assays of PSA according to the magnetic **(c)** washing and **(d)** reaction times.

**Figure 5.** Determination of PSA in PBS solution using magnetic force-assisted electrochemical sandwich immunoassays. (a) Cyclic voltammograms for various concentrations of PSA from 0 to 25 ng/mL. (b) Cathodic peak currents vs. PSA concentration. Mean ± standard deviation ($n \geq 3$). The fitting curve is also plotted ($R^2 = 0.96$).

**Figure 6.** Cyclic voltammograms in the assays of 10 ng/mL PSA in PBS solution, human sera. Anodic and cathodic peaks of gold were observable when NaCl was added to human serum.

**Figure 7.** Determination of PSA in human serum using magnetic force-assisted electrochemical sandwich immunoassays. **(a)** Cyclic voltammograms for various concentrations of PSA from 0 to 25 ng/mL. **(b)** Cathodic peak currents vs. PSA concentration. Mean ± standard deviation ($n \geq 3$). The inset shows a log plot of the data. The fitting curve is also plotted ($R^2 = 0.97$). The limit of detection was calculated to be 0.085 ng/mL.

**Figure 8.** Comparison of the PSA values of 16 patient samples measured by the proposed method with those measured by a reference device, cobas e 801 ($r = 0.997$, $y = 1.04x - 0.124$)

Table 1. Spiked PSA recovery data of the MESIA-based PSA assays

| Added PSA (ng/ml) | Observed PSA (ng/ml) | Recovery (%) |
|---|---|---|
| 1.03 | 1.02 | 99.03 |
| | 1.00 | 97.09 |
| | 1.01 | 98.06 |
| 5.60 | 5.60 | 99.82 |
| | 5.42 | 96.79 |
| | 5.55 | 99.11 |
| 13.24 | 12.98 | 98.04 |
| | 13.21 | 99.77 |
| | 13.32 | 100.6 |
| 24.92 | 24.89 | 99.98 |
| | 24.13 | 96.83 |
| | 25.11 | 100.8 |

Table 2. Precision data for the MESIA-based PSA assays

| Sample number | Mean PSA (ng/ml) | Coefficient of variation (%) | | | |
|---|---|---|---|---|---|
| | | Within-run | Between-run | Between-day | Between-lot |
| 1 | 0.264 | 13.5 | 7.5 | 5.1 | 6.5 |
| 2 | 1.02 | 8.6 | 1.6 | 1.6 | 5.8 |
| 3 | 5.56 | 5.4 | 6.8 | 6.8 | 7.1 |
| 4 | 29.1 | 6.1 | 7.6 | 5.5 | 3.0 |

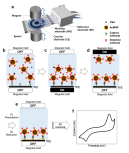

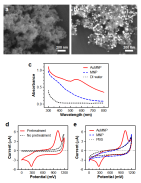

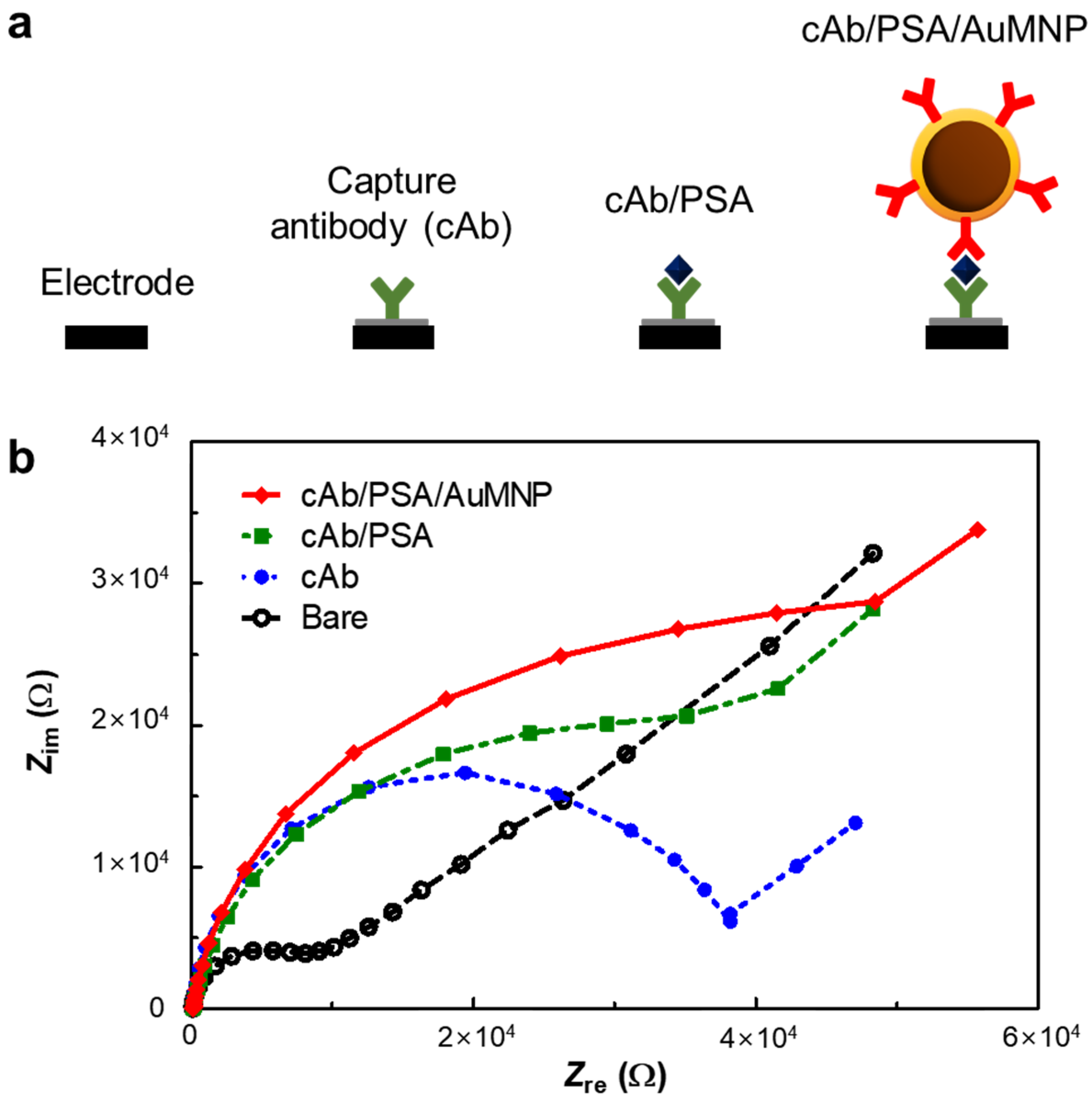
a
cAb/PSA/AuMNP
Capture
antibody (cAb)
cAb/PSA
Electrode
b
cAb/PSA/AuMNP
cAb/PSA
cAb
Bare
$Z_{im}$ (Ω)
$Z_{re}$ (Ω)
0
1×10^4
2×10^4
3×10^4
4×10^4
6×10^4

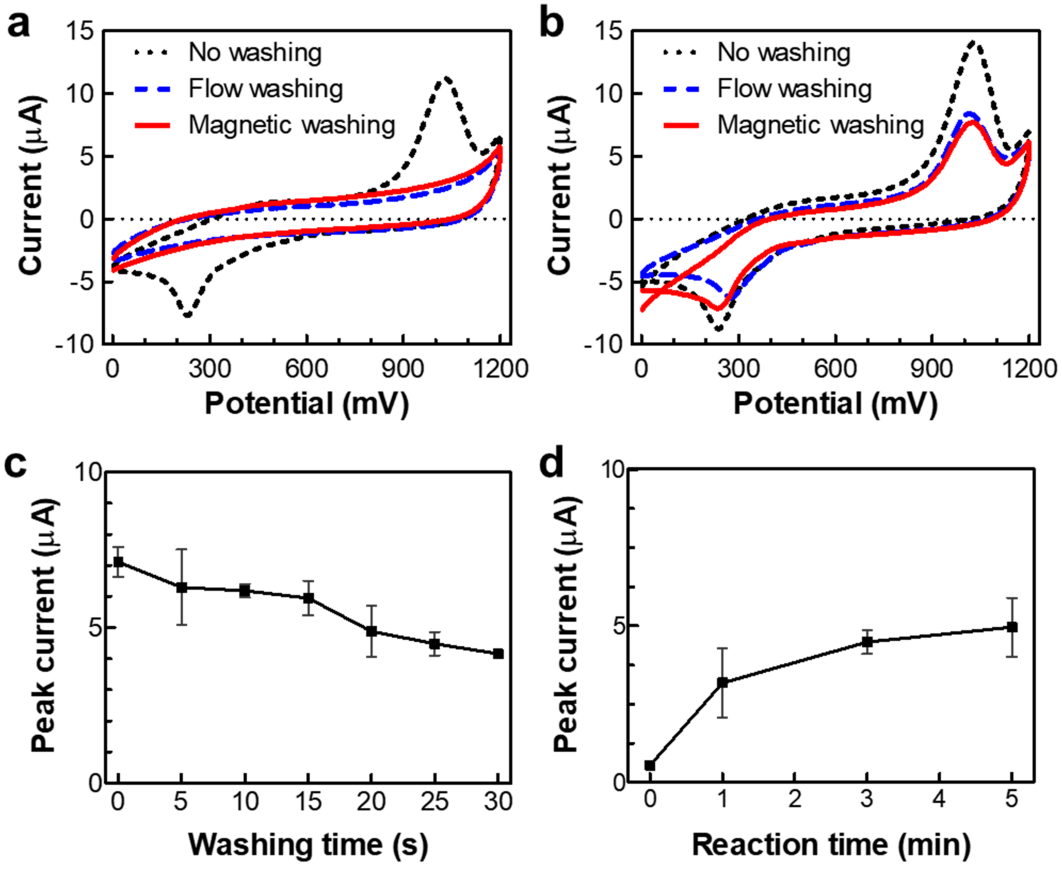

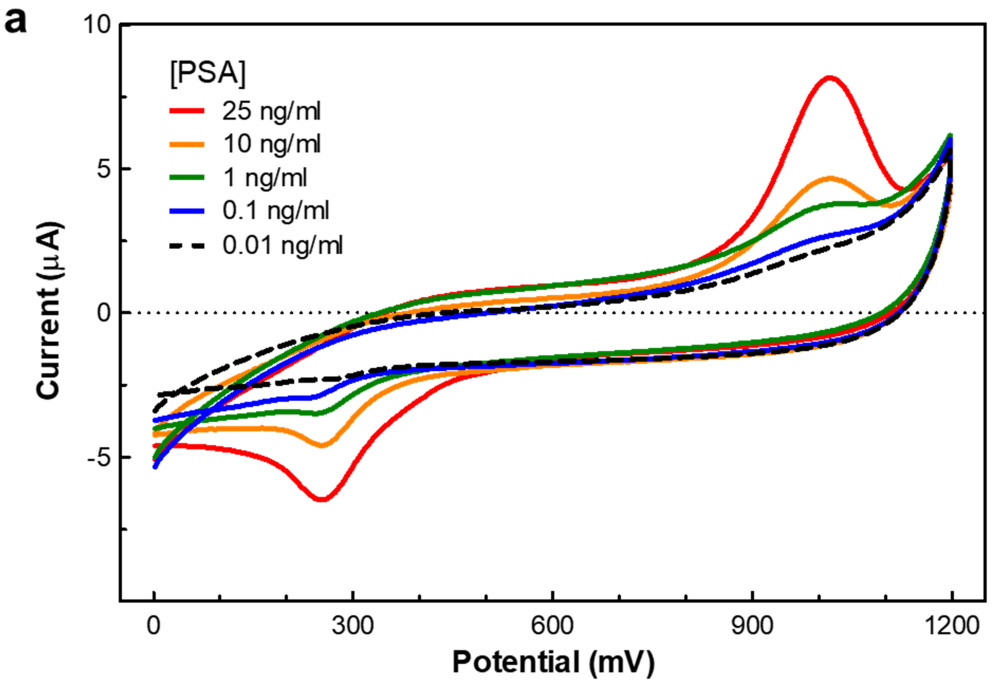
a
[PSA]
25 ng/ml
10 ng/ml
1 ng/ml
0.1 ng/ml
0.01 ng/ml
Current (μA)
Potential (mV)
10
5
0
-5
0
300
600
900
1200

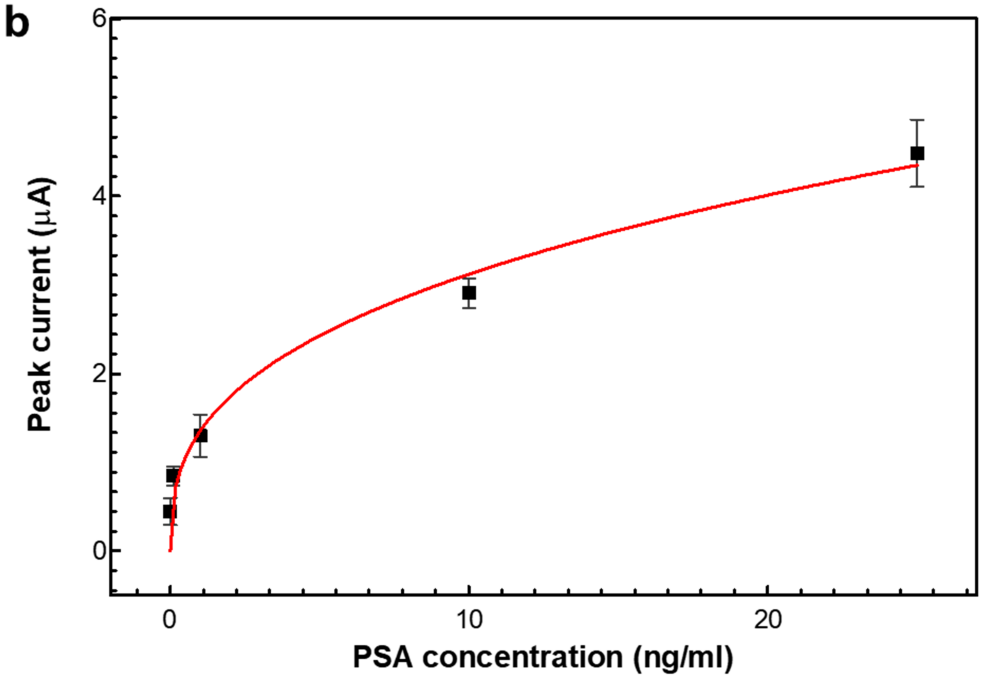
b
Peak current (μA)
PSA concentration (ng/ml)
6
4
2
0
0
10
20

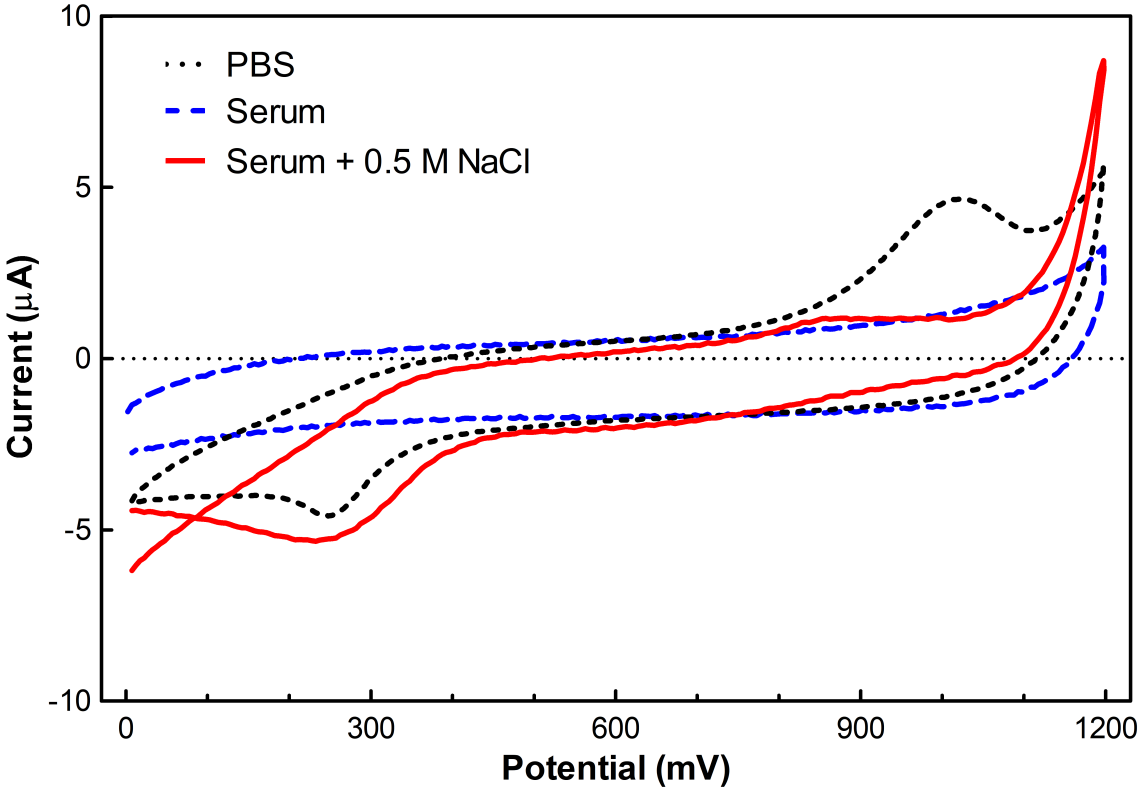

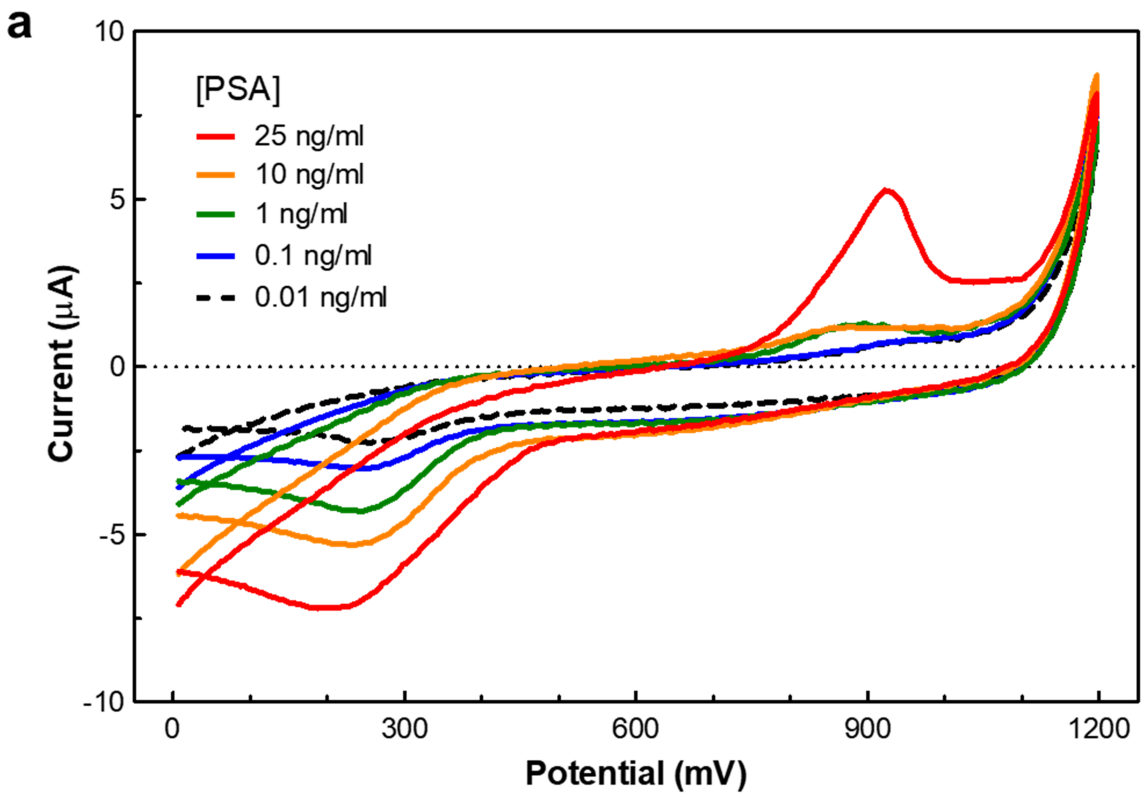
a
[PSA]
25 ng/ml
10 ng/ml
1 ng/ml
0.1 ng/ml
0.01 ng/ml
Current (μA)
Potential (mV)
10
5
0
-5
-10
0
300
600
900
1200

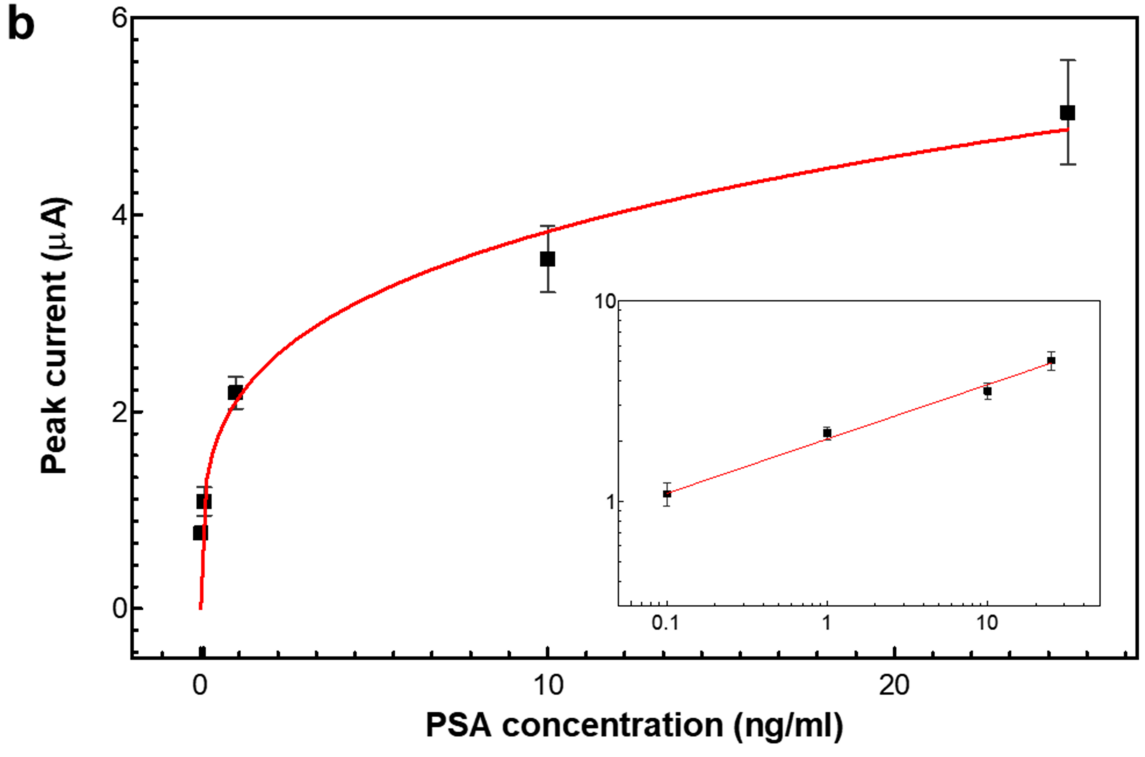
b
Peak current (μA)
PSA concentration (ng/ml)
6
4
2
0
0
10
20
10
1
0.1
1
10

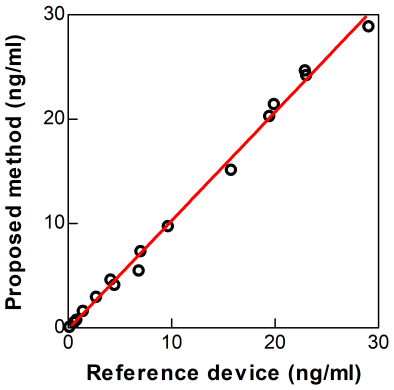

**Highlights:**

- Gold-coated magnetic nanoprobes enable fast and sensitive electrochemical immunoassay
- Prostate-specific antigen in 10 μL of human serum could be determined within 5 min
- Limit of detection of 0.085 ng/ml was achieved using the present technique
- Recovery, reproducibility, and method comparison tests were conducted using patient samples

Declaration of interests

☒ The authors declare that they have no known competing financial interests or personal relationships that could have appeared to influence the work reported in this paper.

☐The authors declare the following financial interests/personal relationships which may be considered as potential competing interests: